J|A|C|S
ARTICLES
Published on Web 02/24/2006

Acid−Base Bifunctional and Dielectric Outer-Sphere Effects in Heterogeneous Catalysis: A Comparative Investigation of Model Primary Amine Catalysts

John D. Bass, Andrew Solovyov, Andrew J. Pascall, and Alexander Katz*

Contribution from the Department of Chemical Engineering, University of California at Berkeley, Berkeley, California 94720-1462

Received October 29, 2005; E-mail: katz@cchem.berkeley.edu

Abstract: Dielectric and acid−base bifunctional effects are elucidated in heterogeneous aminocatalysis using a synthetic strategy based on bulk silica imprinting. Acid−base cooperativity between silanols and amines yields a bifunctional catalyst for the Henry reaction that forms α,β-unsaturated product via quasi-equilibrated iminium intermediate. Solid-state UV/vis spectroscopy of catalyst materials treated with salicylaldehyde demonstrates zwitterionic iminium ion to be the thermodynamically preferred product in the bifunctional catalyst. This product is observed to a much lesser extent relative to its neutral imine tautomer in primary amine catalysts having outer-sphere silanols partially replaced by aprotic functional groups. One of these primary amine catalysts, consisting of a polar outer-sphere environment derived from cyano-terminated capping groups, has activity comparable to that of the bifunctional catalyst in the Henry reaction, but instead forms the β-nitro alcohol product in high selectivity (~99%). This appears to be the first observation of selective alcohol formation in primary amine catalysis of the Henry reaction. A primary amine catalyst with a methyl-terminated outer-sphere also produces alcohol, albeit at a rate that is 50-fold slower than the cyano-terminated catalyst, demonstrating that outer-sphere dielectric constant affects catalyst activity. We further investigate the importance of organizational effects in enabling acid−base cooperativity within the context of bifunctional catalysis, and the unique role of the solid surface as a macroscopic ligand to impose this cooperativity. Our results unequivocally demonstrate that reaction mechanism and product selectivity in heterogeneous aminocatalysis are critically dependent on the outer-sphere environment.

Introduction

Acid−base cooperativity is commonly invoked in enzymatic and catalytic antibody catalysis.[1−7] This paradigm of biological catalysts has inspired the synthesis of homogeneous bifunctional catalysts with superior activity and selectivity, including enantioselectivity, relative to their individual acid and base counterparts.[8−16] However, the function of these homogeneous bifunctional catalysts can strongly depend on the separation distance between acid and base groups.[8,9,16−21] This was illustrated by Swain and Brown, who showed that while 2-hydroxypyridine catalyzes the mutarotation of tetramethylglucose via an acid−base bifunctional mechanism, 3- and 4-hydroxypyridines are 1000-fold less active and exhibit kinetics consistent with general catalysis.[8] Recent work in the synthesis of homogeneous bifunctional catalysts demonstrates a pronounced distance sensitivity for acid−base cooperativity.[8,9,18−21]

A heterogeneous organic−inorganic bifunctional catalyst could, in principle, overcome this sensitivity by providing a near-continuous range of acid−base distances.[19] This could increase bifunctional catalyst versatility by providing various optimal distances for cooperativity, as illustrated in Scheme 1. Such a catalyst would be particularly advantageous for multistep reactions where several kinetically relevant steps have unique distance requirements for acid−base coopertivity. However, to the best of our knowledge, there are no examples of hybrid organic−inorganic materials rigorously proven to act as acid−

(1) Mosier, N. S.; Hall, P.; Ladisch, C. M.; Ladisch, M. R. *Adv. Biochem. Eng./Biotechnol.* **1999**, *65*, 23−40.
(2) Mccarter, J. D.; Withers, S. G. *Curr. Opin. Struct. Biol.* **1994**, *4*, 885−892.
(3) Debler, E. W.; Ito, S.; Seebeck, F. P.; Heine, A.; Hilvert, D.; Wilson, I. A. *Proc. Natl. Acad. Sci. U.S.A.* **2005**, *102*, 4984−4989.
(4) Hoffmann, T.; Zhong, G. F.; List, B.; Shabat, D.; Anderson, J.; Gramatikova, S.; Lerner, R. A.; Barbas, C. F. *J. Am. Chem. Soc.* **1998**, *120*, 2768−2779.
(5) Hennig, M.; Darimont, B. D.; Jansonius, J. N.; Kirschner, K. *J. Mol. Biol.* **2002**, *319*, 757−766.
(6) Kartha, G.; Bello, J.; Harker, D. *Nature* **1967**, *213*, 862−865.
(7) Carter, P.; Wells, J. A. *Nature* **1988**, *332*, 564−568.
(8) Swain, C. G.; Brown, J. F. *J. Am. Chem. Soc.* **1952**, *74*, 2534−2537.
(9) Okino, T.; Hoashi, Y.; Furukawa, T.; Xu, X. N.; Takemoto, Y. *J. Am. Chem. Soc.* **2005**, *127*, 119−125.
(10) Okino, T.; Hoashi, Y.; Takemoto, Y. *J. Am. Chem. Soc.* **2003**, *125*, 12672−12673.
(11) Sakthivel, K.; Notz, W.; Bui, T.; Barbas, C. F. *J. Am. Chem. Soc.* **2001**, *123*, 5260−5267.
(12) List, B. *Synlett* **2001**, 1675−1686.
(13) Wang, W.; Wang, J.; Li, H. *Angew. Chem., Int. Ed.* **2005**, *44*, 1369−1371.
(14) Saito, S.; Yamamoto, H. *Acc. Chem. Res.* **2004**, *37*, 570−579.
(15) Hine, J. *Acc. Chem. Res.* **1978**, *11*, 1−7.
(16) Anslyn, E.; Breslow, R. *J. Am. Chem. Soc.* **1989**, *111*, 8931−8932.
(17) Breslow, R.; Graff, A. *J. Am. Chem. Soc.* **1993**, *115*, 10988−10989.
(18) Hine, J.; Li, W. S. *J. Org. Chem.* **1975**, *40*, 2622−2626.
(19) Hine, J.; Cholod, M. S.; King, R. A. *J. Am. Chem. Soc.* **1974**, *96*, 835−845.
(20) Calter, M. A.; Orr, R. K. *Tetrahedron Lett.* **2003**, *44*, 5699−5701.
(21) Tanabe, K.; Yamaguchi, T. *Catal. Today* **1994**, *20*, 185−198.

Scheme 1. The Silica Surface as a Macroscopic Ligand Providing a Range of Acid−Base Distances for Bifunctional Cooperativity

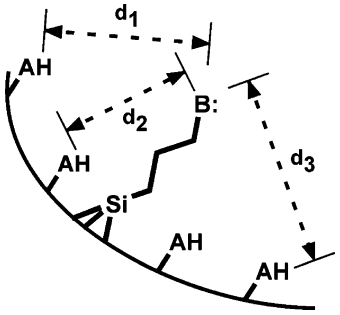

base bifunctional catalysts. This is due to a materials limitation caused by the inability to selectively remove the acid or base component of the active site without concurrently modifying the catalyst structure or the relative positioning of active sites.[21−24] Both bulk structural characteristics[25] and cooperative effects between proximal functional groups[26] can strongly influence catalyst activity. Also, changes to the outer-sphere dielectric environment must be explicitly addressed when selectively removing acid or base components via a materials synthesis strategy. These dielectric effects play an important role in catalysis.[27−33] In biological systems, for example, the outer-sphere dielectric environment created by the hydrophobic protein interior can change the reactivity of primary amines by lowering their pK_a, leading to highly nucleophilic amine groups.[30−33]

Our goal is to assess how the outer-sphere dielectric environment and acid−base cooperativity independently contribute to chemical reactivity. Materials syntheses based on bulk silica imprinting allow us to systematically vary the composition of the outer sphere while keeping other material properties constant. Our approach involves copolymerization of a carbamate imprint with tetraethyl orthosilicate to form hybrid organic−inorganic sol−gel material **1**. Material **1** consists of a silanol-rich polar/acidic mesoporous network that is the direct result of the sol−gel synthesis. It is subsequently modified via capping of silanols to tailor the outer-sphere environment. The isolated active sites remain chemically protected as carbamates during synthesis and capping; thus, changes to the outer-sphere environment do not affect the composition of the ultimate catalytically active primary amine. The nonpolar/nonacidic material, **2**, is synthesized by capping accessible silanols with excess dimethyl butyl chlorosilane. Capping with the size-similar dimethyl cyanopropyl chlorosilane at identical surface coverage yields the polar/nonacidic material **3**. Because these latter two materials are derived from the same parent mesoporous material **1**, the structure of the silica network and the relative positioning of active sites are identical. Carbamates in materials **1**, **2**, and **3** are subsequently thermally deprotected by mild heating to form catalytic materials **4**, **5**, and **6** (Chart 1).[34]

Carbamate-deprotection kinetics provides the first measure of the importance of outer-sphere acid−base cooperativity and dielectric environment on reactivity at the active site. We also use salicylaldehyde as a probe molecule in binding experiments aimed at characterizing outer-sphere acidity and dielectric environment of primary amines in **4**, **5**, and **6**. In addition, materials **4**, **5**, and **6** are used as catalysts for the Michael, Henry, and Knoevenagel reactions. Results are compared to relevant homogeneous models **7** and **8**, which consist of a primary amine tethered to a phenolic oxygen on the lower rim of a calix[4]arene scaffold. Such calix[4]arene triols were shown to be Bronsted acid centers with a pK_a of 6.9;[35] thus, they are a good model for tethered amines on silica, because silanols on silica surfaces have an average pK_a value of 7.1.[36,37] Related calix[4]arene triols show acid−base cooperativity in aldol catalysis,[38] with the length of the amine tether strongly influencing activity.[38] We compare **7** and **8** with catalyst **4** to highlight the role of the heterogeneous surface as an organizational scaffold that enables acid-base bifunctional cooperativity in catalysis. Our results provide new mechanistic insights into primary amine reactivity as controlled by the outer-sphere environment, which are significant given the prevalence of primary amine catalysis, including in biological systems where lysine residues play a central catalytic role.[39,40]

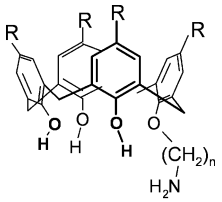

7: R=t-Bu, n=3
8: R=H, n=4

Results and Discussion

Thermolytic carbamate decomposition in materials **1**, **2**, and **3** proceeds via a charge-separated transition state involving protonation of the carbonyl oxygen.[41] Based on this mechanism, both the dielectric environment and the presence of an acidic silanol functionality in the outer sphere should affect thermolysis kinetics. Figure 1 shows the derivative of the weight loss during carbamate thermolysis. The maximum rate of thermolysis for **1**, which contains acidic silanols, occurs at 198 °C, about 46 °C lower than for nonacidic materials **2** and **3**. A smaller

(22) Iglesia, E.; Barton, D. G.; Biscardi, J. A.; Gines, M. J. L.; Soled, S. L. *Catal. Today* **1997**, *38*, 339−360.
(23) Tanabe, K. *J. Chin. Chem. Soc.* **1998**, *45*, 597−602.
(24) Yamaguch, T.; Sasaki, H.; Tanabe, K. *Chem. Lett.* **1973**, 1017−1018.
(25) Macquarrie, D. J.; Maggi, R.; Mazzacani, A.; Sartori, G.; Sartorio, R. *Appl. Catal., A* **2003**, *246*, 183−188.
(26) Dufaud, V.; Davis, M. E. *J. Am. Chem. Soc.* **2003**, *125*, 9403−9413.
(27) Thorn, S. N.; Daniels, R. G.; Auditor, M. T. M.; Hilvert, D. *Nature* **1995**, *373*, 228−230.
(28) Kemp, D. S.; Cox, D. D.; Paul, K. G. *J. Am. Chem. Soc.* **1975**, *97*, 7312−7318.
(29) Harris, T. K. T., G. J. *Life* **2002**, *53*, 85−98.
(30) Urry, D. W. P., S. Q.; Parker, T. M.; Gowda, D. C.; Harris, R. D. *Angew. Chem., Int. Ed. Engl.* **1993**, *32*, 1440−1442.
(31) Urry, D. W. G., D. C.; Peng, S. Q.; Parker, T. M.; Harris, R. D. *J. Am. Chem. Soc.* **1992**, *114*, 8716−8717.
(32) Karlstrom, A. Z., G.; Rader, C.; Larsen, N. A.; Heine, A.; Fuller, R.; List, B.; Tanaka, F.; Wilson, I. A.; Barbas, C. F.; Lerner, R. A. *Proc. Natl. Acad. Sci. U.S.A.* **2000**, *97*, 3878−3883.
(33) Barbas, C. F. H., A.; Zhong, G.; Hoffmann, T.; Gramatikova, S.; Bjornestedt, R.; List, B.; Anderson, J.; Stura, E. A.; Wilson, I. A.; Lerner, R. A. *Science* **1997**, *278*, 2085−2092.
(34) Bass, J. D.; Katz, A. *Chem. Mater.* **2003**, *15*, 2757−2763.
(35) Araki, K.; Iwamoto, K.; Shinkai, S.; Matsuda, T. *Bull. Chem. Soc. Jpn.* **1990**, *63*, 3480−3485.
(36) Hair, M. L.; Hertl, W. *J. Phys. Chem.* **1970**, *74*, 91−94.
(37) Marshall, K.; Ridgewel, G.; Rocheste, C.; Simpson, J. *Chem. Ind.* **1974**, 775−776.
(38) Liu, L.; Yang, Z. X.; Wang, Y. L.; Chen, S. H. *Chin. Chem. Lett.* **2000**, *11*, 485−488.
(39) Jencks, W. P. *Annu. Rev. Biochem.* **1963**, *32*, 639−676.
(40) Speck, J. C.; Rowley, P. T.; Horecker, B. L. *J. Am. Chem. Soc.* **1963**, *85*, 1012−1013.
(41) Ashcroft, S. J.; Thorne, M. P. *Can. J. Chem.* **1972**, *50*, 3478−3487.

Chart 1

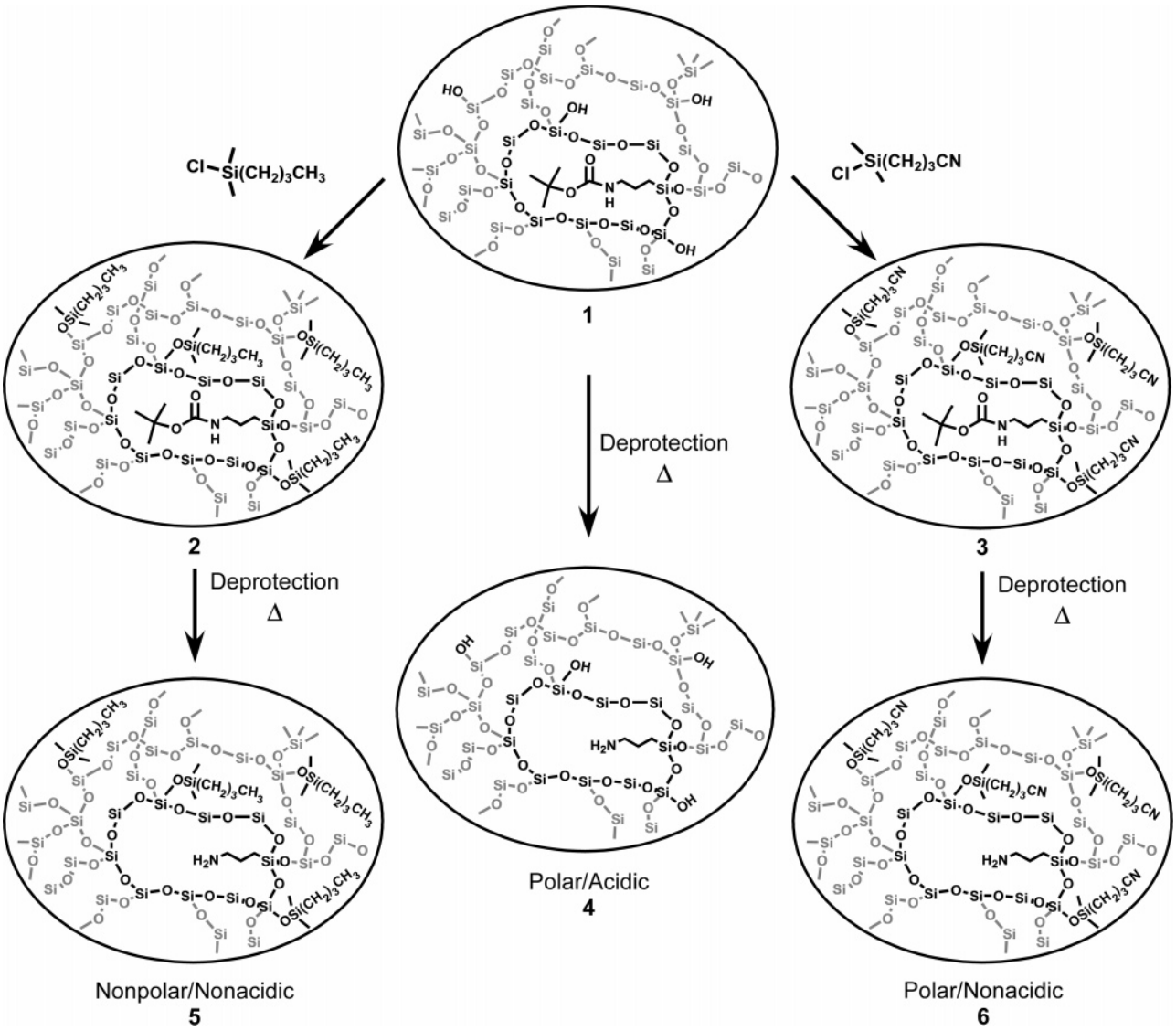

difference caused by dielectric effects is apparent in the slightly lower thermolysis temperature of **3** versus **2**. Importantly, only a homogeneous population of sites is observed for each material. This is observed by a single event in the TGA trace during deprotection (the deviation from a first-order trace for **1** is observed due to minor weight loss from desorption of physisorbed water). This indicates that the majority of active sites within each material experience the same outer-sphere environment. Such a uniform site distribution suggests single-site behavior and allows us to draw conclusions about the entire population of active sites in the reactivity studies below.

Activation energies for carbamate thermolysis in materials **1**, **2**, and **3** were calculated from TGA data using the method of Redhead[42] (Table 1) at conditions where the rate of reaction was limited solely by chemical kinetics.[43] Assuming a value for the frequency factor of 10^{13} s^{-1}, the activation energies were measured to be 26.7 ± 0.1, 29.9 ± 0.15, and 29.4 ± 0.15 kcal/mol for **1**, **2**, and **3**, respectively. The slightly lower activation energy for carbamate thermolysis in the polar/nonacidic **3** as compared to nonpolar/nonacidic **2** is attributed to the higher dielectric environment in the outer-sphere capable of stabilizing charge separation in the transition state. Acidity has a larger effect, decreasing the activation barrier for carbamate thermolysis in **1** by 2.7 kcal/mol. For this to occur, acidic silanols must be present in the outer sphere in a position to interact with the carbonyl group during thermolysis (Scheme 2). The lower activity for thermolysis of **2** and **3** relative to **1** is not due to a general lack of silanols in these materials. Total organic content via combustion analysis shows that capping consumes 1.1 mmol/g of silanols on the surface. This represents 30% of the silanols shown to be in **1** by infrared spectroscopy (Supporting Information). Thus, most silanols remain unreacted during capping of **1** in synthesis of **2** and **3**, and the total number of silanols remains in greater than 10-fold excess relative to carbamate, with remaining silanols less active for facilitating thermolysis, as reflected by the greater activation energy for materials **2** and **3**.

We used the site-directed probe salicylaldehyde to investigate the acidity and dielectric effects of the outer-sphere environment

(42) Redhead, P. A. *Vacuum* **1962**, *12*, 203−211.
(43) No variations were observed using heating rates of 0.5−5 °C/min. Larger particles (30−150 μm) were compared to smaller (<30 μm) and mixed batches and were found to give equal values.

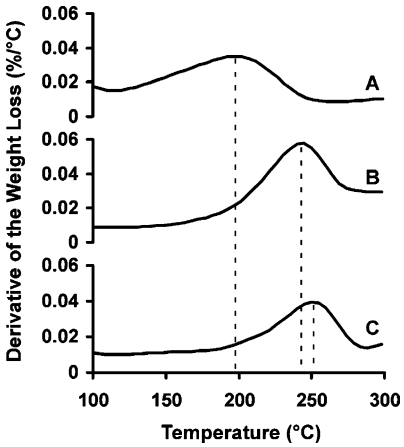

Figure 1. Thermal gravimetric analysis of carbamate deprotection in materials **1**, **2**, and **3**. The temperature of the maximum thermolysis rate is significantly lower in the polar/acidic **1** (A) at 198 °C as compared to the polar/nonacidic **3** (B) at 244 °C and the nonpolar/nonacidic material **2** (C) at 251 °C. N_2 flow of 20 mL min^{-1} with a programmed heating rate of 1 °C per min.

Table 1. Kinetics of Immobilized Carbamate Deprotection via Thermolysis

material	temperature at maximum rate of thermolysis[a]	activation energy[b]
1	198 °C	26.7 ± 0.1 kcal/mol
2	251 °C	29.9 ± 0.15 kcal/mol
3	244 °C	29.4 ± 0.15 kcal/mol

[a] Heating rate of 1 °C per min. [b] Based on the method of Redhead,[42] frequency factor assumed as 10^{13} s^{-1}; error analysis on the basis of the variation in the measured data.

Scheme 2. Thermolytic Deprotection of the Carbamate Protecting Group Is Facilitated in the Presence of Acidic Silanols[a]

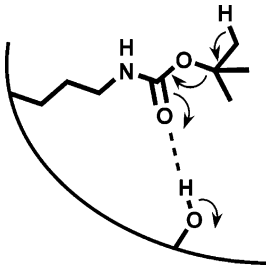

[a] The silanols must have the correct geometrical orientation relative to the carbamate functional groups to facilitate the reaction.

surrounding primary amines in materials **4**, **5**, and **6**, as well as in homogeneous models **7** and **8**. The condensation of primary amines with salicylaldehyde can form two tautomeric products: a neutral phenolic imine with an absorption band at 310−350 nm and a zwitterionic tautomer that absorbs at 400−450 nm.[34,44] Figure 2 shows the diffuse reflectance UV/visible spectra of **4**, **5**, and **6** after contact with salicylaldehyde. The strong band at 400 nm represents the zwitterionic iminium tautomer resulting from the outer-sphere acidity in **4**. In **5** and **6**, this band is much weaker than that at 315 nm representing the neutral phenolic form of the imine. Acidic silanols in material **4** must be present within the outer sphere of the active site so as to hydrogen bond to the phenolic oxygen to form

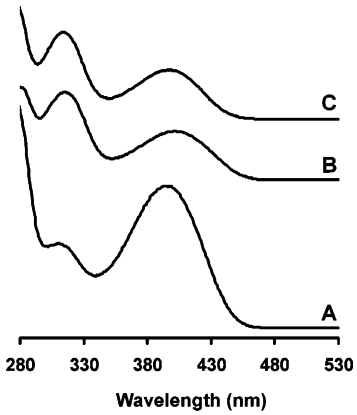

Figure 2. Solid-state diffuse-reflectance UV/visible spectra of (A) polar/acidic catalyst **4**, (B) nonpolar/nonacidic catalyst **5**, and (C) polar/nonacidic catalyst **6** after reaction with salicylaldehyde to form a solvochromatic indicator. The indicator in **4** shows a pronounced zwitterion band near 400 nm due to the acidic silanols. The upper two spectra show a strong band from the phenolic form at 315 nm of the indicator. Data are represented in Kubelka Munk units.

Scheme 3. The Reaction between Salicylaldehyde and a Primary Amine Can Form (A) the Zwitterionic Iminium Tautomer in the Presence of Acidic Silanols as in **4** or (B) the Neutral Imine in the Absence of Acidic Silanols as in **5** and **6**

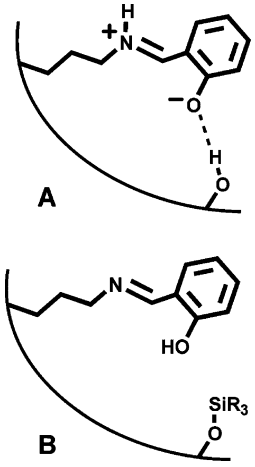

zwitterionic iminium tautomer in Scheme 3. Note that by using a slightly different materials synthesis recipe for sol−gel hydrolysis and condensation, we have previously prepared a material similar in composition to **4** that showed even less neutral phenolic relative to zwitterionic contribution in Figure 2A.[44] Thus, this product ratio can vary depending on subtle differences in the materials synthesis procedure, further illustrating the importance of deriving all materials from the same parent material. (For this reason, our procedures are reported in detail in the Supporting Information.)

These results are consistent with previous studies with imines derived from salicylaldehyde in homogeneous media. The zwitterionic iminium tautomer was observed on dissolution in acidic protic solvents, such as highly fluorinated alcohols, and in aprotic solvents the neutral phenolic product was favored.[45−47] For salicylideneaniline, the stability of the zwitterionic species has been correlated to the Kamlet−Taft solvent parameter α, which relates to the H-bond donating ability of the solvent.[47]

(44) Bass, J. D.; Anderson, S. L.; Katz, A. *Angew. Chem., Int. Ed.* **2003**, *42*, 5219−5222.
(45) Casades, I.; Alvaro, M.; Garcia, H.; Pillai, M. N. *Eur. J. Org. Chem.* **2002**, 2074−2079.
(46) Turbeville, W.; Dutta, P. K. *J. Phys. Chem.* **1990**, *94*, 4060−4066.
(47) Dutta, P. K.; Turbeville, W. *J. Phys. Chem.* **1991**, *95*, 4087−4092.

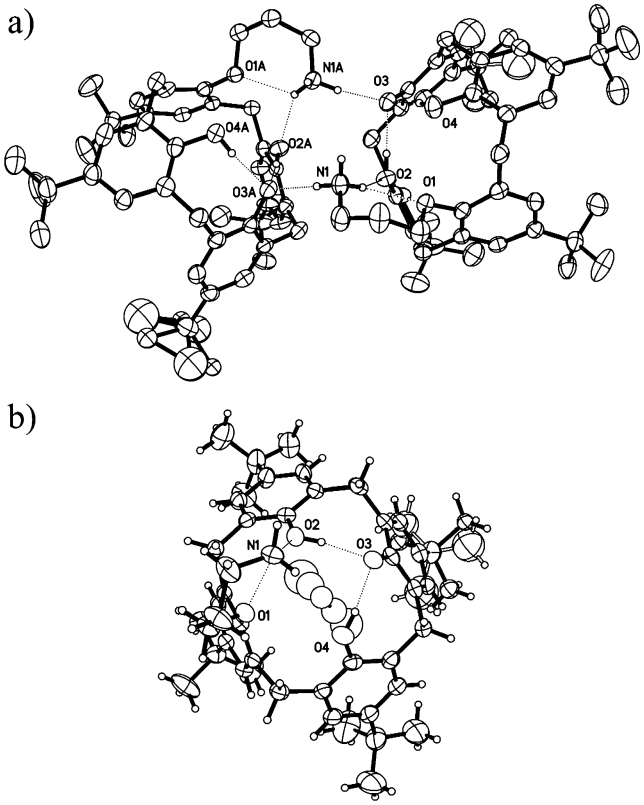

Figure 3. Structure of the homogeneous acid−base analogue **7** showing (a) the organized dimer and (b) the hydrogen-bonding pattern within a monomer unit comprising the dimer in (a). The dimer is held together by a strong intermolecular interaction between the primary ammonium cation and the phenolate anion on oxygen O(3) of the calixarene lower rim.

No correlation was previously observed for the parameter Π*, which relates to the ability of a solvent to stabilize charge via dielectric effects,[47] which is consistent with the same observed preference for the neutral phenolic form in materials **5** and **6**.

The spectra in Figure 2 demonstrate that the dielectric environment in the nonpolar/nonacidic **5** is lower than in polar materials **4** and **6**. The wavelength maximum of the zwitterionic band of the bound chromophore undergoes a hypsochromic shift of 6 nm from the nonpolar **5** (402 nm) to the polar materials **4** and **6** (both at 396 nm). This shift is typical of $\pi-\pi^*$ transitions in zwitterionic species, because the excited state has a smaller dipole moment than the ground state.[48] This decreases the energy required for excitation in nonpolar **5** relative to the polar materials **4** and **6**.

The acid−base bifunctional nature of the homogeneous models **7** and **8** can be hypothesized on the basis of the known acidity of lower rim calix[4]arene triols[16] and the interactions of such acidic OH nests with primary amines.[49−51] The acid−base bifunctional nature is also observed in the single-crystal X-ray diffraction structure of **7** (Figure 3). During structure refinement, the ammonium and hydroxyl hydrogens atoms were located in a difference Fourier map and included in their observed positions normalized to standard N−H and O−H distances. No peaks were observed near the phenolate oxygen O(3). The calixarenes, in the cone conformation, are held together in pairs by strong hydrogen bonds between the primary ammonium cations and the phenolate anions on the adjacent calixarene. The distance from N(1) to O(3) on the adjacent calixarene in the dimer is 2.65(4) Å, and one of the ammonium protons lies near the N−O vector. In a pattern differing markedly from the typical pattern observed in other monosubstituted calix[4]arenes without base substituents,[35] two intramolecular hydrogen bonds from O(2) and O(4) to O(3) are observed. The O−O distance is 2.58(5) Å for each, and the located hydrogen atoms lie along the corresponding vectors. There is also a moderately strong bifurcated intramolecular hydrogen bond from the ammonium N(1) to the phenol oxygen O(2) (N−O distance = 2.90(3) Å) and to O(1) (N−O distance = 2.79(5) Å). These results show an acidic, hydrogen-bonded phenol triol that has protonated the primary amine, allowing the formation of strong intermolecular and intramolecular hydrogen-bonding interactions.

Evidence for acid−base cooperativity in the homogeneous models **7** and **8** upon reaction with salicylaldehyde was investigated. Phenolic imines **9** and **10** were isolated upon treatment of **7** and **8** with salicylaldehyde. These imines, despite retaining the acidic phenolic triol, show no zwitterionic tautomer in aprotic solvents (Figure 4). Only upon solvation in a highly protic environment does the zwitterion tautomer become favored as a result of intermolecular solvent interactions. Comparing these results with the heterogeneous acid−base bifunctional material **4** treated with salicylaldehyde confirms the importance of the silanol-rich silica surface as a macroscopic acidic ligand that presents the primary amines with a continuous acidic surface for facilitating acid−base cooperativity.

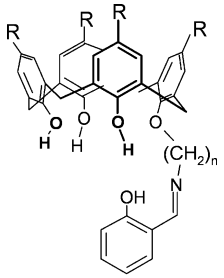

9: R=t-Bu, n=3
10: R=H, n=4

We next examine probe reactions with turnovers to investigate outer-sphere effects on primary amine catalysis. The Michael addition of malononitrile to β-nitrostyrene is catalyzed by general bases via an ion-pair mechanism (Scheme 4), where the function of the general base is to deprotonate the malononitrile to form carbanion intermediates.[52] The results of this reaction under anhydrous conditions are shown in Figure 5. The higher activity of **6** over **5** (a factor of 7) is consistent with the ability of a high-dielectric outer-sphere environment to facilitate ion-pair formation and charge separation in the transition state.

Acid−base bifunctional effects were examined independently from outer-sphere dielectric contributions on catalysis using the Henry reaction as a probe. We hypothesize that the Henry reaction may potentially proceed via two mechanisms: an imine mechanism (Scheme 5) and an ion-pair mechanism (Scheme

(48) Reichardt, C. *Chem. Rev.* **1994**, *94*, 2319−2358.
(49) El Nahhal, I. M.; Chehimi, M. M.; Cordier, C.; Dodin, G. *J. Non-Cryst. Solids* **2000**, *275*, 142−146.
(50) Yang, J. J.; ElNahhal, I. M.; Chuang, I. S.; Maciel, G. E. *J. Non-Cryst. Solids* **1997**, *209*, 19−39.
(51) Horr, T. J.; Arora, P. S. *Colloids Surf., A* **1997**, *126*, 113−121.
(52) Carey, F. A.; Sundberg, R. J. *Advanced Organic Chemistry, Part B*, 3rd ed.; Plenum Press: New York, 1990.

Scheme 4. Ion-Pair Mechanism of Catalysis by Amine-Functionalized Silica for the Michael Reaction

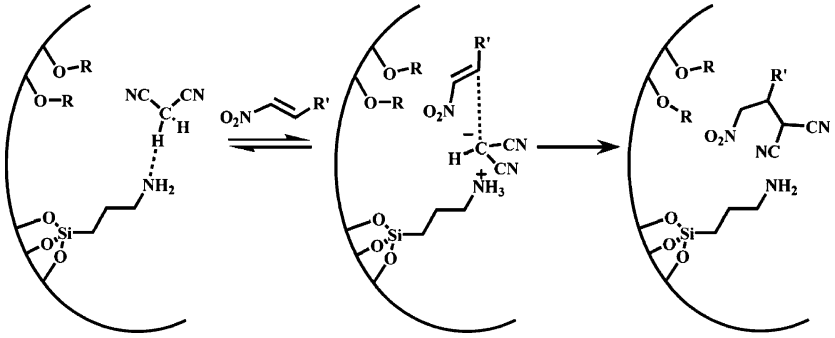

6). The mechanism involving covalent imine intermediates is reported to account for primary amine catalysis in homogeneous[53−55] and enzymatic[39,40] systems. In this mechanism, both imine formation[15,56,57] and imine protonation to form iminum ions[55,58] are promoted by acid−base bifunctionality. Formation of an iminum ion, as in the salicylaldehyde study above, creates a carbon center that is significantly more electrophilic than the carbonyl compound.[52,55,58] This facilitates attack by the carbon nucleophile during Henry catalysis.

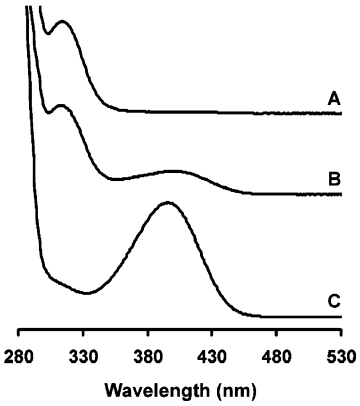

Figure 4. UV/visible spectra of the homogeneous acid−base analogue **9** in three different solvents showing absorbance (au) as a function of wavelength. In acetonitrile (A), the imine exists in the phenolic form, despite being pendent to an acidic species. The zwitterionic tautomer is only formed in strongly hydrogen bond donating solvents, being fractionally present in methanol (B), and predominant in pentafluoro-1-propanol (C). Similar results are obtained for the calixarene **10** that contains a four-carbon tether. The concentration is 60 μM.

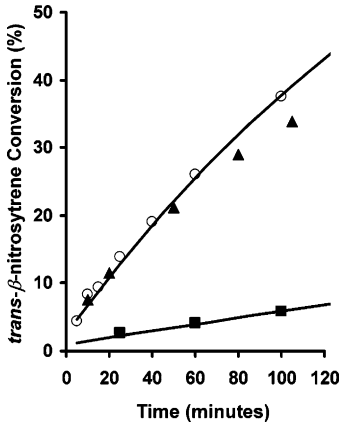

Figure 5. Conversion of *trans*-β-nitrostyrene for its base-catalyzed Michael addition with malononitrile. The high dielectric catalyst **6** (▲) exhibits a 7-fold higher activity as compared to the nonpolar catalyst **5** (■). This rate enhancement is due to the changes in the outer-sphere dielectric environment surrounding the amine active site. Data for catalyst **4** (○) are also shown as well as solid lines fitting to a first-order kinetics model for **4** and **5**. The yield of the 2-cyano-4-nitro-3-phenylbutyronitrile product at 100% nitrostyrene conversion via ^{1}H NMR was 96% ± 3% using catalyst **6**.

In the presence of bases for which imine formation is kinetically unfavorable, we postulate that the Henry reaction may produce the β-nitro alcohol product via an ion-pair mechanism. This mechanism has been proposed previously[59−61] for primary amine catalysis on silica, but it has remained unproven. Crucially, because the olefin and alcohol products do not interconvert under reaction conditions,[62] the product distribution directly reflects the reaction mechanism: the α,β-unsaturated product forms via the imine mechanism (Scheme 5) and the β-nitro alcohol via the ion-pair mechanism (Scheme 6).

The Henry reaction of nitromethane and 4-nitrobenzaldehyde on catalysts **4**, **5**, and **6** shows a marked, and unprecedented, reversal in selectivity between the polar/acidic catalyst **4** and the polar/nonacidic catalyst **6**. These kinetic data, measured using ^{1}H NMR spectroscopy, are shown in Figure 6. In catalyst **4**, acid−base bifunctional cooperativity among silanols and the primary amines results in a lower barrier for imine formation and the selective formation of product **11**. This product is formed at a rate that is 30-fold greater than for the nonacidic catalysts **5** and **6**. The observed zero order kinetic dependence on aldehyde reactant concentration up to nearly 90% conversion of aldehyde indicates that imine formation is quasi-equilibrated and energetically favored during catalysis, leading to saturation of active sites for catalyst **4**.

In stark contrast with the acid−base bifunctional imine mechanism on catalyst **4**, catalyst **6** favors instead the ion-pair mechanism and forms the β-nitro alcohol **12** with 99% selectiv-

(53) Westheimer, F. H.; Cohen, H. *J. Am. Chem. Soc.* **1938**, *60*, 90−94.
(54) Spencer, T. A.; Neel, H. S.; Flechtne, T.; Zayle, R. A. *Tetrahedron Lett.* **1965**, 3889−3897.
(55) Crowell, T. I.; Peck, D. W. *J. Am. Chem. Soc.* **1953**, *75*, 1075−1077.
(56) Hine, J.; Cholod, M. S.; Chess, W. K. *J. Am. Chem. Soc.* **1973**, *95*, 4270−4276.
(57) Hine, J.; Via, F. A. *J. Org. Chem.* **1977**, *42*, 1972−1978.
(58) Santerre, G. M.; Hansrote, C. J.; Crowell, T. I. *J. Am. Chem. Soc.* **1958**, *80*, 1254−1257.
(59) Angeletti, E.; Canepa, C.; Martinetti, G.; Venturello, P. *J. Chem. Soc., Perkin Trans. 1* **1989**, 105−107.
(60) Choudary, B. M.; Kantam, M. L.; Reddy, C. V.; Rao, K. K.; Figueras, F. *Green Chem.* **1999**, *1*, 187−189.
(61) Huh, S.; Chen, H. T.; Wiench, J. W.; Pruski, M.; Lin, V. S. Y. *J. Am. Chem. Soc.* **2004**, *126*, 1010−1011.
(62) Interconversion was ruled out by conducting the following experiments under dry conditions. (1) Reaction in the presence of **6** and subsequent filtration and transfer via syringe to **4** after 60% conversion of aldehyde (54% yield of **12**). No decrease in **12** was observed after 4 h exposure to **4** and aldehyde conversion to 90%. (2) The reverse catalyst sequence using identical methods with filtration and transfer at 20% aldehyde conversion (13% yield of **11**). No decrease in **11** was observed after 5.5 h exposure to **6** and aldehyde conversion to 50%.

Scheme 5. Imine Catalytic Mechanism for the Production of the Dehydrated Product for the Henry Reaction (with Nitromethane) Catalyzed by Amines on Silica[a]

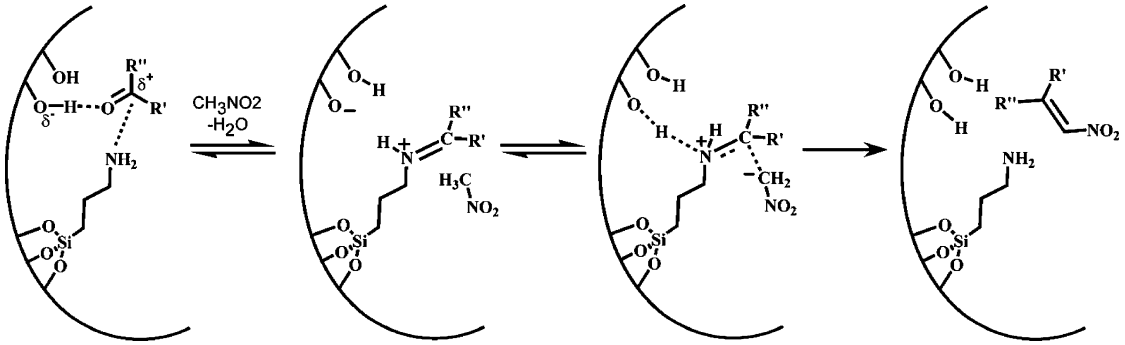

[a] Both the imine formation step and the attack of the nucleophile on the imine are known to be acid catalyzed.

Scheme 6. Ion-Pair Mechanism of Catalysis by Amine-Functionalized Silica for the Production of β-Nitro Alcohol Product in the Henry Reaction

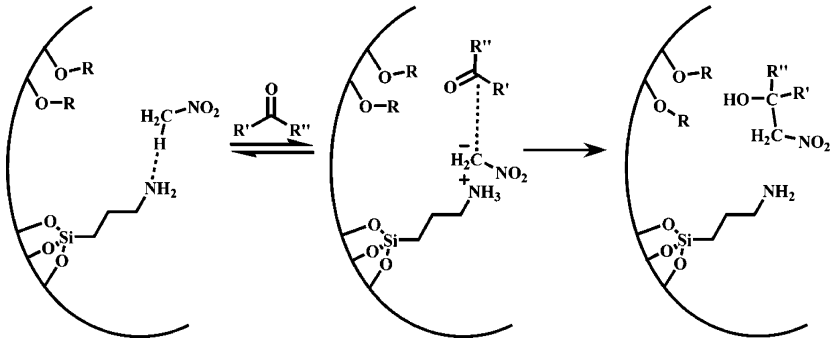

ity. As in the Michael reaction, dielectric effects play a significant role in promoting the ion-pair pathway for the Henry reaction on nonacidic materials. The rate of formation of β-nitro alcohol on **6** is ~50 times greater than that on **5**. This again reflects a high local dielectric environment that stabilizes ion pair formation and charge separation in the transition state. The generality of these trends above was investigated by using a commercial 3-aminopropyl-functionalized material for the same Henry reaction. This hybrid material consists of a dense monolayer of 3-aminopropyl groups on silica (1.3 mmol/g). We have previously shown that the outer-sphere surrounding the amine active sites in this material behaves as a nonacidic material for related condensation reactions.[44] The absence of acid sites due the displacement of silanols with the 3-aminopropyl modifier has been measured using X-ray photoelectron spectroscopy.[49−51] This catalyst forms mainly product **12**, but with lower selectivity to product **12** (85% at 20% conversion) and at a 4-fold lower rate per amine than catalyst **6** under identical conditions.

Our demonstration that primary amines can function as general base catalysts for synthesizing products via an ion-pair mechanism is unique, in lifht of all previous observations of primary amine catalysis via imine intermediates in both homogeneous[53−55] and enzymatic[39,40] systems. A postulated[59−61] ion-pair mechanism for amine on silica materials remains to be demonstrated,[63,64] and, to the best of our knowledge, preference for ion-pair mechanisms over condensation mechanisms is shown here for the first time for a primary amine catalyst. Our results demonstrate that the reaction mechanism depends critically on the outer-sphere environment surrounding the immobilized primary amine. Outer-sphere acidity creates an active pathway to dehydrated products via imine formation, while the polar/nonacidic outer-sphere environment of material **6** creates a primary amine that is active and selective for product formation via ion-pair mechanisms.

Materials **4**, **5**, and **6** are all active catalysts for Knoevenagel condensation of aldehydes with activated methylene compounds (Table 2). Previously, we observed large effects of up to 2 orders of magnitude difference for the polar/acidic environment found in catalyst **4** relative to a material that was capped with nonpolar/nonacidic trimethylsilyl chloride (similar to material **5**);[44] however, the origin of these effects (dielectric versus acid−base bifunctional) remained unclear. In this report, we performed the Knoevenagel condensation of malononitrile with 3-nitrobenzaldehyde on **4**, **5**, and **6**. Here, the alcohol product is expected to be unstable under reaction conditions because of the strength of electron-withdrawing groups in the malononitrile adduct, leading to the same olefin product in both imine and ion-pair mechanisms.

The results of the Knoevenagel condensation between 3-nitrobenzaldehyde and malononitrile on catalysts **4**, **5**, and **6** are shown in Figure 7. Reactions were conducted under anhydrous conditions to avoid kinetic complications caused by water (vide infra) by adding dehydrated mesoporous silica as a minimally catalytic desiccant. This also keeps the total number of acidic silanols in the reaction constant for catalysts **5** and **6** (no silica was added for catalysis with **4**). In this way, all reactions contain the same active functional groups and differ only in their

(63) Lasperas, M.; Llorett, T.; Chaves, L.; Rodriguez, I.; Cauvel, A.; Brunel, D. *Heterog. Catal. Fine Chem. IV* **1997**, *108*, 75−82.
(64) Demicheli, G.; Maggi, R.; Mazzacani, A.; Righi, P.; Sartori, G.; Bigi, F. *Tetrahedron Lett.* **2001**, *42*, 2401−2403.

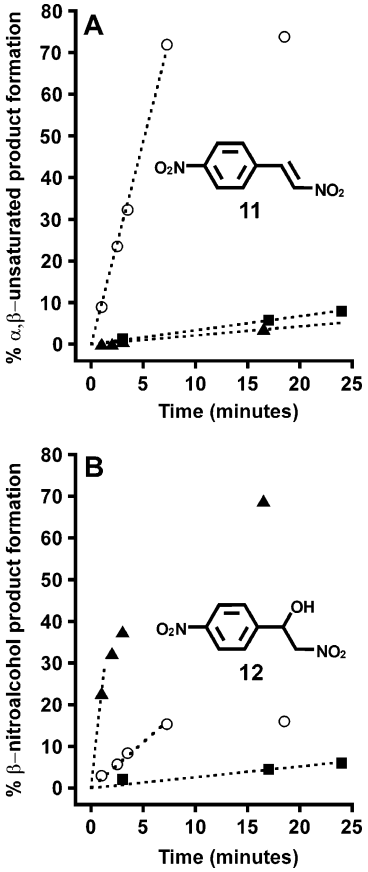

Figure 6. Product formation for the Henry reaction between 4-nitrobenzaldehyde and nitromethane. Outer-sphere differences between the acidic catalyst **4** (○) and the nonacidic catalysts **5** (■) and **6** (▲) lead to significant effects in the observed selectivity with catalyst **4** producing predominantly (4:1) α,β-unsaturated product **11** (A) at a rate 30-fold higher than the nonacidic catalysts. The formation of the β-nitro alcohol product **12** (B) is sensitive to the dielectric environment, comparing **5** to **6**, where the rate increases by a factor of 50 in the more polar material. The combined product yield per aldehyde reacted was 95% ± 5% for all catalysts studied. Dashed lines show the initial TOF.

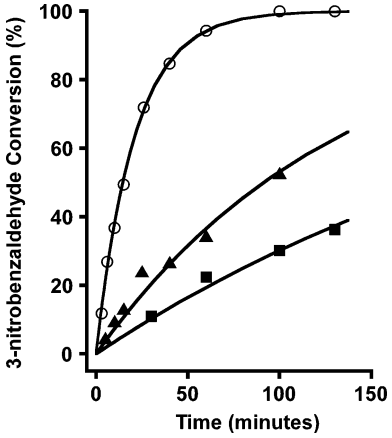

Figure 7. The fractional conversion of 3-nitrobenzaldehyde as a function of time for the base-catalyzed Knoevenagel condensation with malononitrile. Outer-sphere differences between the acidic catalyst **4** (○) and the nonacidic catalysts **5** (■) and **6** (▲) lead to significant effects in the observed rate of reaction. The principal cause of the rate acceleration in **4** results from the presence of acidic silanols acting in concert with the amine in an acid−base bifunctional mechanism. The rate difference between polar/nonacidic **6** and the nonpolar/nonacidic **5** shows the secondary effect of the dielectric environment. Solid lines represent first-order kinetic models with respect to 3-nitrobenzaldehyde concentration.

Table 2. Summary of Catalysis for Michael, Henry, and Knoevenagel Reactions under Dry Conditions

material	Michael k_{app}[a]	Knoevenagel k_{app}[a]	Henry product ratio[b] [TOF][b]
4	0.27	2.9	80:20 [12]
5	0.03		40:60 [0.6]
5 and silica[c]		0.22	
6	0.23		1:99 [22]
6 and silica[c]		0.48	
silica[d]		0.13	0:100
cyano capped silica[d]	0		[0]

[a] h^{-1}, using $-dC_{aldehyde}/dt = k_{app}C_{aldehyde}$; at low conversion for Michael reaction. [b] Ratio of dehydrated to alcohol product (30% aldehyde conversion), TOF: initial number of reaction events h^{-1} amine site^{-1}. [c] Mesoporous silica as desiccant; an equivalent number of silanols as **1** was added. [d] Materials treated like they have the equivalent number of amines as the corresponding imprinted catalyst; dehydrated at 250 °C for 4 h prior to reaction.

organization of these groups. The dehydrated mesoporous silica itself contributes less than 5% to overall catalytic rate for catalyst **4**.

Comparing catalysts **5** and **6** in Figure 7 shows that dielectric effects increase the rate ~3-fold. However, the effect of the acidic silanol groups in **4** is more significant, increasing the rate by an additional 8-fold over **6** (22-fold faster than **5**). The lower rate in **5** and **6** reflects the removal of the acid functionality, which, in turn, eliminates acid−base bifunctional cooperativity. Like in the Henry reaction, the role of the acidic functional groups in **1** is to divert the reaction through the imine mechanism via bifunctional catalysis, yielding a higher rate. These observations again illustrate how acid−base organization controls bifunctional catalysis, even in heterogeneous systems, as all reactions contain the same quantity of amines and silanols.

Mass transport effects were ruled out by similar Knoevenagel reaction rates with large (30−150 μm) and small (<30 μm) particles.[65] Any potential blocking effects of the capping groups in preventing amine active site accessibility by virtue of their steric bulk were also ruled out. Because such effects would not appear in a particle size variation experiment, we synthesized the nonpolar/nonacidic catalyst **13** using the capping agent trimethyl chlorosilane. Molecular modeling shows that this capping group is 40% smaller than the dimethyl butyl chlorosilane used to synthesize the nonpolar/nonacidic catalyst **5**. Weight loss in thermogravimetric analysis shows that materials **5** and **13** have identical capping efficiencies of 1.1 mmol/g (this is also true for **6**). This consistency reflects our ability to minimize differences between materials via the synthesis procedures used, which becomes possible because all materials are derived from the same parent material **1**. With an equivalent fraction of OH groups capped, only the steric bulk at the surface is different, being significantly smaller in **7** than in **5**. Despite this difference in steric bulk at the surface, the materials behaved identically for Knoevenagel catalysis (see Supporting Information) and have nearly identical activation energies for thermolysis (30.1 ± 0.2 kcal/mol for **13**). Also, materials **5** and **6**, which differ in the molecular size of the capping group by less than 5%, showed marked differences in catalytic behavior for all three model reactions. Taken together, these results demonstrate that any changes in steric bulk at the catalyst surface caused by

(65) This is the fastest reaction studied in this Article and would be most sensitive to these effects. These data, along with representative SEM pictures, are available in the Supporting Information.

Table 3. Summary of Catalysis for Michael, Henry, and Knoevenagel Reactions under Ambient Conditions

material	Michael k_{app}[a]	Knoevenagel k_{app}[a]	Henry product ratio[b] [TOF][b]
4	0.35	2.0	85:15 [10]
5	0.006	0.026	68:32 [0.6]
6	0.024	0.1	60:40 [1.2]

[a] h^{-1}, using $-dC_{aldehyde}/dt = k_{app}C_{aldehyde}$; at low conversion for Michael reaction. [b] Ratio of dehydrated to alcohol product (25% aldehyde conversion), TOF: initial number of reaction events h^{-1} amine $site^{-1}$.

immobilized capping agent do not affect catalysis and are inconsequential for active site accessibility.

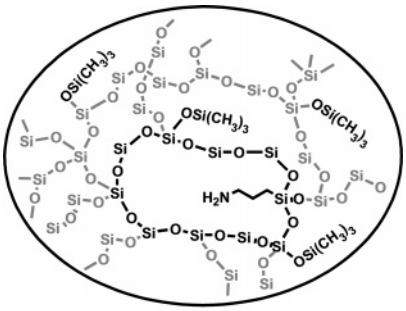

Nonpolar/Nonacidic
13

The acid−base cooperativity demonstrated in material **4** requires a diverse range of structural requirements between the bound amine intermediate and the acidic silanols acting on it. Such versatility is in stark contrast with the specificity of acid−base distances generally observed in homogeneous systems.[8−10,15,38] Likewise, homogeneous catalysts **7** and **8** did not show acid−base cooperativity in the form of bifunctional catalysis, exhibiting catalytic activities comparable to *n*-butylamine.[66] This highlights the important role of the silica surface in organizing acid-base functional groups for bifunctional catalysis and shows that the simple presence of acid and base functions in stoichiometric proportions and close proximity on the same molecule is insufficient for acid−base cooperativity in catalysis.

Small amounts of water in the reaction mixture have a dramatic effect on the observed catalysis proceeding via ion-pair mechanisms, but a negligible effect on catalysis occurring via acid−base bifunctional mechanisms. This effect can be observed simply by using materials that have been stored in the presence of atmospheric moisture instead of catalysts that are dehydrated before reaction, and amounts to less than 10 wt % of water for all catalysts as measured by thermogravimetric analysis, which is less than that required to fill the pores of the catalyst with water. For materials equilibrated with ambient moisture before use in Knoevenagel catalysis, the rate enhancement of **4** is 20-fold over **6** and 75-fold over **5**. This effect is not confined to the Knoevenagel reaction, but is general for all three catalytic reactions. These data are summarized in Table 3. These marked rate and selectivity differences between acidic and nonacidic catalysts reflect a lower rate on nonacidic materials upon exposure to water, while the activity of **4** remains essentially unchanged for all three reactions. This is particularly pronounced for **6**, for which the rate decreases by an order of magnitude for both the Michael and the Henry reactions relative to anhydrous conditions. Also important is the concomitant change in selectivity observed in the Henry reaction for material **6** between anhydrous and wet conditions. This decreases from a greater than 99% selectivity for product **11** under anhydrous conditions to a selectivity of 40% when small amounts of water are present. Thus, the decrease in rate of β-nitro alcohol product formation under wet conditions in **6** is about 50-fold and indicates that the presence of water specifically inhibits the ion-pair mechanism. This inhibition is likely to arise from competitive protonation of the amine by water in these materials, as protonation of amines on silica by water after exposure to humid air has been observed previously.[67] From the perspective of the imine mechanism in the acidic environment of material **4**, the protonation state of the amine remains unchanged by addition of small amounts of water, because the amine is already protonated due to the acidity of the surface. This protonation of the amine in material **4** is not a significant barrier to efficient catalysis due to the overall favorable acid−base cooperativity, which synthesizes imine rapidly under bifunctional conditions[15,56,57] and favors the strongly electrophilic iminium ion tautomer as observed in our salicylaldehyde binding results. We further note that the effect of water in the Henry reaction is self-promoting. Water disfavors the ion-pair mechanism relative to the imine mechanism, which, unlike the ion-pair mechanism, produces water during reaction. The presence of small amounts of water therefore leads to further water synthesis during Henry catalysis, due to promotion of the imine over ion-pair mechanism.

Conclusions

We utilize a materials synthesis approach for elucidating the independent contributions of outer-sphere dielectric environment and acid−base cooperativity on primary amine reactivity in a heterogeneous hybrid organic−inorganic catalyst. In the Henry reaction, these two outer-sphere properties are critical in determining both the rate and the mechanism of the reaction. While both polar materials facilitate catalysis by at least 20-fold over the nonpolar catalyst **5**, they show opposite product selectivity. Because of the rapid formation of the highly electrophilic iminium cation intermediate, the acid−base bifunctional material **4** follows a zero-order dependence on aldehyde reactant concentration on its catalytic rate and is highly selective for the α,β-unsaturated product **11**. In contrast, the polar/nonacidic material **6** facilitates catalysis through a noncovalent ion-pair mechanism due to its high dielectric environment and the lack of acidity in the outer sphere. This translates into a measured selectivity of 99% for the β-nitro alcohol product **12**. The synthesis of an active primary amine catalyst that facilitates products via an ion-pair mechanism selectively over imine-derived products has not been observed for primary amine catalysts previously. Supporting evidence for the mechanisms above is provided by solid-state UV/vis spectroscopy on salicylaldehyde treated catalysts **4**−**6**. The spectrum of salicylaldehyde-treated bifunctional catalyst **4** contains a predominant band that is due to the strong thermodynamic preference for forming iminium zwitterionic tautomer in this

(66) For the Knoevenagel reaction, k_{app} for **7** and *n*-butylamine was less than 0.01 h^{-1}, using $-dC_{aldehyde}/dt = k_{app}C_{aldehyde}$.

(67) Allen, G. C.; Sorbello, F.; Altavilla, C.; Castorina, A.; Ciliberto, E. *Thin Solid Films* **2005**, *483*, 306−311.

material, and a minor band due to neutral imine tautomer. In general catalysts **5** and **6** after salicylaldehyde treatment, there is reversal in the order of intensity of these two bands.

Outer-sphere environment effects are further manifested in carbamate thermolysis, where the acid−base bifunctional material lowers the activation barrier by 2.7 kcal/mol while only a small dielectric effect of 0.5 kcal/mol is observed. Catalysis in the Michael and Knoevenagel reactions echo the Henry results with the high dielectric materials being more active than the nonpolar material **5**. In the presence of water, however, only the acid−base bifunctional material **4** performs well compared to anhydrous conditions, resulting in an order of magnitude or higher activity in comparison with **5** and **6** for all catalytic reactions. This is due to the depressed catalytic rate in the nonacidic materials for the ion-pair mechanism, as manifested in changes in the Henry reaction selectivity, likely due to competitive protonation by water. The remarkably diverse set of reactions affected by acid−base bifunctional cooperativity observed in this Article, including the various catalytic probe reactions, zwitterion formation during salicyladehyde binding, and immobilized carbamate thermolysis, is testament to the promiscuity of acid−base distances attainable in heterogeneous hybrid organic−inorganic catalysts. These data prove the concept hypothesized in Scheme 1, relating to the silica surface providing a range of acid−base distances for bifunctional cooperativity. In contrast, no evidence was observed for bifunctional cooperativity in homogeneous calixarene models despite the presence of acidic groups juxtaposed to a pendent amine. Altogether, our results are significant for understanding acid−base bifunctional reactivity in heterogeneous organic−inorganic catalysts, as well as the chemical reactivity of heterogeneous primary amine catalysts.

Experimental Section

General. All reagents were purchased from Aldrich at analytical grade and used as received, unless otherwise noted. 3-Cyanopropyldimethylchlorosilane was distilled prior to use. Dry solvents were prepared via distillation using standard methods. ^{1}H NMR spectra were recorded in $CDCl_3$ (293 K) either on a Bruker AV-300 (300 MHz) instrument or on an AVB-400 (400 MHz) instrument. Single-crystal diffraction data were collected at the UC Berkeley College of Chemistry X-ray Crystallographic Facility. All catalytic reactions were conducted in a well-ventilated fume hood. FAB-MS spectra were recorded using a *o*-nitrophenyl octyl ether (NPOE) matrix at the UC Berkeley Mass Spectrometry Facility.

Michael Addition. A typical reaction was conducted using about 10 mg of catalyst (the amount of catalyst was fixed at 0.02 molar equivalents of amine relative to *trans*-β-nitrostyrene) in 8 mL of an anhydrous benzene solution of concentration 0.022 M in *trans*-β-nitrostyrene and 0.044 M of malononitrile. Catalysts were prepared via thermolysis (Supporting Information) in the reactor vessel (volume was 10 mL) prior to addition and kept air free under a N_2 environment. The reaction was performed at room temperature (22 °C), and aliquots were taken by syringe and analyzed by gas chromatography using 1,3,5-trimethoxybenzene as an internal standard.

Henry Reaction. Reactions were conducted using approximately 30 mg of catalyst (the amount of catalyst was fixed at 0.01 molar equivalents of amine relative to 4-nitrobenzaldehyde). Catalysts were prepared via thermolysis (Supporting Information) in the reactor vessel (volume was 10 mL) prior to addition and kept air free under a N_2 environment. To this vessel was added a solution containing 5 mmol nitromethane, 0.5 mmol 4-nitrobenzaldehyde, and 0.05 mmol nitrobenzene as an internal standard. The reaction was performed at 40 °C. Conversion and selectivity were determined via ^{1}H NMR by taking aliquots via syringe filter and diluting with $CDCl_3$. Resonances: 5.6 ppm (β-nitro alcohol product), 7.5 ppm (nitrobenzene), 7.72−7.74 ppm (α,β-unsaturated product), and 10.1 ppm (4-nitrobenzaldehyde).

Knoevenagel Condensation. A typical reaction was conducted using about 10 mg of catalyst (the amount of catalyst was fixed at 0.01 molar equivalents of amine relative to 3-nitrobenzaldyde) in 8 mL of an anhydrous benzene solution of concentration 0.022 M in 3-nitrobenzaldyde and 0.044 M of malononitrile. To capped catalysts was added mesoporous silica (Selecto) as a minimally catalytic desiccant in a ratio that kept the total number of acidic silanols in the reaction constant. Catalysts were prepared via thermolysis (Supporting Information) in the reactor vessel (volume was 10 mL) prior to reactant addition and kept air free under a N_2 environment. The reaction was performed at room temperature (22 °C), and aliquots were taken by syringe and analyzed by gas chromatography using 1,3,5-trimethoxybenzene as an internal standard.

Synthesis of NBoc Protected Calixarenes 7 and 8 via Mitsunobu Reaction. To a mixture of calix[4]arene (0.154 mmol) and NBoc-alcohol (0.23 mmol) in 5 mL of THF was added triphenyl phosphine (0.23 mmol). The resulting mixture was cooled to 0 °C, and diethylazodicarboxylate (0.23 mmol) as 40% solution in toluene was added dropwise. After 10 min of stirring, the resulting yellow-green solution was allowed to warm to room temperature. After 24 h of stirring at room temperature, the solution was evaporated to dryness and the residue was treated with 2 mL of methanol for 20 min followed by evaporation. Purification via column chromatography yielded the final products.

5,11,17,23-Tetra-(*tert*-butyl)-25-[3-(*tert*-Butoxycarbonylamino)-propoxy]-calix[4]arene-26,27,28-triol (Nboc7). After separation by column chromatography (CH_2Cl_2/methanol = 1:0.025 v/v, R_f 0.4), white powder was obtained in 55% yield: ^{1}H NMR (400 MHz) δ 10.24 (s, 1H, OH), 9.67 (s, 2H, OH), 7.13 (s, 2H, ArH), 7.12 (d, 2H, 2.0 Hz, ArH), 7.10 (s, 2H, ArH), 7.04 (d, 2H, 2.4 Hz, ArH), 5.80 (s, 1H, NH), 4.31, 4.33 (two d, 2H+2H, 13.2 Hz, $ArCH_2Ar$), 4.19 (t, 2H, 6.0 Hz, OCH_2), 3.64 (m, 2H, CH_2N), 3.49 (d, 4H, 13.2 Hz, $ArCH_2Ar$), 2.35 (m, 2H, OCH_2CH_2), 1.52 (s, 9H, $OC(CH_3)_3$), 1.27 (s, 9H, $C(CH_3)_3$), 1.26 (s, 18H, $C(CH_3)_3$), 1.23 (s, 9H, $C(CH_3)_3$).

25-[4-(*tert*-Butoxycarbonylamino)butoxy]-calix[4]arene-26,27,28-triol (Nboc8). After separation by column chromatography (CH_2Cl_2/methanol = 1:0.02 v/v, R_f 0.6), white powder was obtained in 50% yield: ^{1}H NMR (400 MHz) δ 9.74 (s, 1H, OH), 9.72 (s, 2H, OH), 7.04, 7.06, 7.10, 7.12 (four d, 2H+2H+2H+2H, 7.6 Hz, ArH-*m*), 6.91 (t, 1H, 7.6 Hz, ArH-*p*), 6.72 (t, 1H, 7.6 Hz, ArH-*p*), 6.71 (t, 2H, 7.6 Hz, ArH-*p*), 4.85 (s, 1H, NH), 4.31, 4.38 (two d, 2H+2H, 12.8 Hz, $ArCH_2Ar$), 4.20 (t, 2H, 6.8 Hz, OCH_2), 3.50, 3.51 (two d, 2H+2H, 12.8 Hz, $ArCH_2Ar$), 3.40 (m, 2H, CH_2N), 2.21 (m, 2H, OCH_2CH_2), 1.97 (m, 2H, CH_2CH_2N), 1.57 (s, 9H, $OC(CH_3)_3$).

Deprotection of Nboc-Calixarenes. To a solution of NBoc-protected calixarenes (0.09 mmol) in 3.0 mL of dry dichloromethane was added trifluoroacetic acid (0.9 mmol) at 0 °C. The solution was allowed to warm to room temperature and then stirred an additional 10 h. The reaction mixture was then hydrolyzed using a saturated $NaHCO_3$ solution. The aqueous solution was extracted with CH_2Cl_2 and dried over Na_2SO_4. After evaporation of solvent, residue was washed with hexane to give desired calixarene-amines **7** and **8**.

5,11,17,23-Tetra-(*tert*-butyl)-25-[3-aminopropoxy]-calix[4]arene-26,27,28-triol (7). White powder was obtained in 98% yield: ^{1}H NMR (400 MHz) δ 9.00 (br s, 3H+2H, OH+NH_2), 7.07 (s, 2H, ArH), 7.00 (s, 4H, ArH), 6.97 (s, 2H, ArH), 4.13 (m, 4H+2H, $ArCH_2Ar$+OCH_2), 3.51 (m, 2H, OCH_2N), 3.35, 3.39 (two d, 13.6 Hz, $ArCH_2Ar$), 2.43 (m, 2H, OCH_2CH_2), 1.23 (s, 18H, $C(CH_3)_3$), 1.20 (s, 9H, $C(CH_3)_3$), 1.13 (s, 9H, $C(CH_3)_3$). FAB MS *m*/*z* 706.6 [M + H^+].

25-[4-Aminobutoxy]-calix[4]arene-26,27,28-triol (8). White powder was obtained in 95% yield: ^{1}H NMR (400 MHz) δ 7.50 (br s, 3H+2H, OH+NH_2), 6.94−7.06 (m, 8H, ArH), 6.58−6.83 (m, 4H,

ArH), 4.24, 4.28 (two d, 2H+2H, 13.2 Hz, $ArCH_2Ar$), 3.99 (t, 2H, 7.6 Hz, OCH_2), 3.42 (d, 4H, 13.2 Hz, $ArCH_2Ar$), 2.99 (t, 2H, 7.6 Hz, CH_2N), 2.08 (m, 2H, OCH_2CH_2), 1.87 (m, 2H, NCH_2CH_2). MS ES *m*/*z* 496.3 [M + H^+].

General Procedure for Preparation of Calixarene-Imines (9,10). The solution of calixarene amine **7** (or **8**) (0.014 mmol) and salicylaldehyde (0.017 mmol) in 2 mL of *m*-xylene was refluxed over molecular sieves for 10 h. The organic solvent was evaporated, and the residue was washed with hexane. Hexane was separated, and the precipitate formed was dried in a vacuum (0.05 Torr) for 3 h.

5,11,17,23-Tetra-(*tert*-butyl)-25-[3-(2-hydroxyphenylmethylenimino)propoxy]-calix[4]arene-26,27,28-triol (9). Yellow powder was obtained in 98% yield: ^{1}H NMR (400 MHz) δ 14.20 (s, 1H, *o*-HOC_6H_4), 10.24 (s, 1H, OH), 9.64 (s, 2H, OH), 8.73 (s, 1H, CHN), 7.18, 7.35, 7.60 (three m, 1H each, C_6H_4), 7.05−7.15 (br m, 8H, ArH), 6.92 (m, 1H, C_6H_4), 4.33, 4.36 (two d, 2H + 2H, 13.6 Hz, $ArCH_2Ar$), 4.23 (m, 4H, OCH_2+NCH_2), 3.47, 3.51 (two d, 2H+2H, 13.6 Hz, $ArCH_2Ar$), 2.57 (m, 2H, OCH_2CH_2), 1.28 (s, 9H, $C(CH_3)_3$), 1.26 (s, 18H, $C(CH_3)_3$), 1.23 (s, 9H, $C(CH_3)_3$). FAB MS m/z 810.5 [M+H^+].

25-[4-(2-Hydroxyphenylmethylenimino)-propoxy]-calix[4]arene-26,27,28-triol (10). Yellow powder was obtained in 96% yield: ^{1}H NMR (400 MHz) δ 13.44 (s, 1H, *o*-HOC_6H_4), 9.72 (s, 1H, OH), 9.40 (s, 2H, OH), 8.53 (s, 1H, CHN), 7.33 (m, 2H, C_6H_4), 7.00−7.15 (br m, 8H, ArH), 6.92 (m, 2H, C_6H_4), 6.72 (m, 4H, ArH), 4.29, 4.38 (two d, 2H+2H, 13.5 Hz, $ArCH_2Ar$), 4.24 (m, 2H, OCH_2), 3.90 (m, 2H, NCH_2), 3.51 (d, 4H, 13.5 Hz, $ArCH_2Ar$), 2.27 (m, 4H, OCH_2-CH_2+NCH_2CH_2).

Acknowledgment. Funding from the National Science Foundation is gratefully acknowledged (CTS 0407478). A.J.P. is grateful to the Robert and Colleen Haas Scholars Program for a fellowship. The authors thank Dr. Frederick Hollander and Dr. Allen Oliver of the UC Berkeley CHEXRAY facility for determining the structure of **7** via single-crystal X-ray diffraction; Mr. Justin M. Notestein for technical assistance with FTIR spectroscopy; and Ms. Karen Magid for technical assistance with SEM.

Supporting Information Available: Supplementary figures referenced in the text, silica synthesis, capping procedures, thermolysis conditions, salicylaldehyde binding procedures, activation energy measurements, and X-ray crystallographic information (CIF). This material is available free of charge via the Internet at http://pubs.acs.org.

JA057395C